Journal of Building Engineering 95 (2024) 110238

Contents lists available at ScienceDirect

Journal of Building Engineering

journal homepage: www.elsevier.com/locate/jobe

Structural behavior of stone cantilever stairs: Strain monitoring under controlled loading and numerical modeling

Antonio Maria D'Altri [a, b, *], Yolanda Jin [b], Jessica Chen [b], Tiffany Agyarko [b], Guy Nordenson [c, d], Branko Glisic [b]

[a] Department of Civil, Chemical, Environmental, and Materials Engineering, University of Bologna, Italy
[b] Department of Civil and Environmental Engineering, Princeton University, USA
[c] School of Architecture, Princeton University, USA
[d] Guy Nordenson and Associates, New York, USA

ARTICLE INFO

Keywords:
Stone cantilever staircase
Spiral stairs
Structural health monitoring
Fiber optic strain sensor
Finite element model

ABSTRACT

In this paper, the structural behavior of a stone cantilever (or cascade) staircase is investigated through an integration of strain monitoring and numerical modeling. The originality of this work is in the first ever application of this combined approach, where numerical modeling is integrated with actual strain measures on a historic cantilever staircase subjected to controlled loading. The main challenge is indeed modeling a complex staircase geometry together with unknown actual boundary conditions. The Museum of the City of New York staircase, composed of marble treads, is used as case study. Fiber-optic sensors are installed in the intrados of a representative tread. Experimental strain data are collected under human loads, with different loading schemes. A 3D solid finite element model of the staircase, where each tread interacts with the adjacent ones through contact, is used to simulate the loading cases. Various boundary conditions are considered and compared with the experimental data, allowing to identify the most plausible actual boundary condition of the treads. Experimental strain data and numerical results show a good agreement. Consequently, new insights on the structural behavior of stone cantilever stairs and their outstanding structural performance are gathered.

1. Introduction

Stone cantilever stairs are a magnificent example of cultural heritage structures. They are composed of a sequence of monolithic stone treads anchored to the wall on one end only, although each tread supports the one above it. Thus, the term "cantilever" is incorrect from a structural point of view, and some have proposed to call them "cascade stairs" reflecting the load path of vertical shears from tread to tread [1]. Nonetheless, it has been commonly used since the XIV century to refer to stairs with a free end [2]. Stone cantilever stairs can be found in historical buildings with either a straight or spiral arrangement on flat or curved walls, respectively (Fig. 1). Typically, the stone treads may have a rectangular ("unrebated treads") or triangular ("rebated treads") cross-section [3]. In particular, the latter forms a smooth and plain underside ("soffit") of the staircase. The embedment of treads within the wall is typically around 10–15 cm, i.e., significantly shorter than the length of the treads, which can reach 2 m, making these stairs remarkably impressive.

* Corresponding author. Department of Civil, Chemical, Environmental, and Materials Engineering, University of Bologna, Italy.
E-mail address: am.daltri@unibo.it (A.M. D'Altri).

https://doi.org/10.1016/j.jobe.2024.110238
Received 2 April 2024; Received in revised form 5 July 2024; Accepted 16 July 2024
Available online 17 July 2024

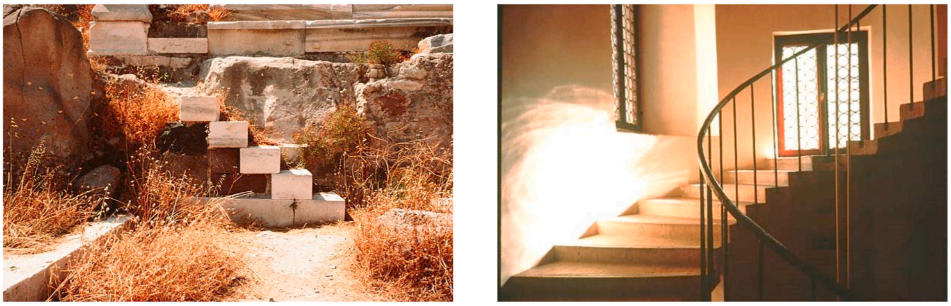

Fig. 1. Stone cantilever stairs. Left: example of straight unrebated treads found in Milos, Greece. Right: example of spiral Palladio's stair at the Academia in Venice, Italy.

The earliest surviving examples of stone cantilever stair, according to [4], can be found in the Cyclades, Greece, and were constructed between 500 and 300 BCE (see an example in Fig. 1, left). Stone cantilever stairs were famously reintroduced by Andrea Palladio (see, e.g., Fig. 1, right), and they became a standard form of construction in Europe from the XVI century [5]. Hence, many examples of stone cantilever stairs can be found all over the world, and most of them are still in use today.

In order to preserve stone cantilever stairs for future generations [6], as well as assess their structural safety (as they are currently utilized and the loads might be increased due to changed intended uses), advanced structural analysis approaches [7,8] have been lately developed to get structural insights on these fascinating structures. Indeed, common engineering practice tools are unusable for this kind of structure.

A very simplified solution to the problem was firstly proposed by Heyman [9], although limited to cantilever stairs of modest flight. The structural analysis of thin shell spiral staircases by means of trust network analysis has been firstly conducted by Block [10]. A more advanced solution based on a rigid no-tension shell model has been proposed by Angelillo [11,12], with a focus on both masonry [11] and monolithic block [12] stairs. This approach allowed studying the equilibrium of staircases based on purely compressive stress fields. Such no-tension shell model has been also applied to a tuff masonry spiral vault with a central pillar in [13]. Another solution based on the assumption that a series of space linear arches, which represent elliptical helixes confined by the exterior wall, bear the load has been proposed in [14]. The effects of concentrated loads on open-well masonry spiral stairs have been investigated in [15]. Additionally, a method to evaluate the effects of potential settlements on masonry helical stairs has been introduced in [16].

Although such solutions are rigorous [17], they are based on several mechanical hypotheses which might be difficult to remove to generalize the problem solutions. In this context, numerical strategies [18–22], and in particular contact-based approaches [23–25], might be an appealing choice to generalize the solutions for stone cantilever stairs, as they are able to deal with complex geometries and boundary conditions, as well as potential defects. One first step forward in this direction has been made in [3], where the discrete element method (DEM) has been employed to perform virtual experiments, evaluating the mechanical behavior of straight and spiral staircases under deadload, live loads and settlements. Additionally, parametric DEM simulations on cantilever spiral staircases have been recently discussed in [2], with the hypothesis of solid rigid treads, allowing for the investigation of a wide range of structural behaviors possible between the fixed and simply supported conditions of the treads. Despite the significant advancements in the analysis of the structural behavior of stone cantilever stairs, none of the existing structural analysis approaches has been somehow validated against real structures, e.g., utilizing actual experimental measurements.

In this paper, the structural behavior of a stone cantilever staircase is investigated through an integration of strain monitoring and numerical modeling. The originality of this work consists in the novel integration of numerical modeling with actual strain measures on a historic cantilever staircase, with unknown actual boundary conditions, subjected to controlled loading. The Museum of the City of New York staircase, composed of marble treads, is used as case study. Fiber-optic sensors, almost invisible to the naked eye, were installed in the intrados of a representative tread. Experimental stain data are collected under moving human loads, with different loading schemes. Then, a 3D finite element model of the entire staircase, where each tread interacts with the adjacent ones through contact-based interactions, is used to simulate the loading cases. Various boundary conditions are assumed and compared with the experimental data. Strain monitoring under controlled loading and the application of the same load sequence to the numerical model allows indeed a straightforward comparison.

This paper is structured as follows. Section 2 presents the research aim of this study. Section 3 describes the case study, the sensors set-up, the loading conditions, as well as the numerical modeling adopted to simulate the staircase. Section 4 shows the results and discusses the comparison between experimental and numerical outcomes. Section 5 discusses the conclusions of this study.

2. Research aim

This study represents the very first contribution integrating advanced numerical modeling with actual strain measures on a real stone cantilever staircase, with unknown actual boundary conditions, subjected to controlled loading. The research aim is to shed light on true structural behavior of these complex structures. To achieve this aim it is thus fundamental to validate quantitatively the numerical model through experimental data. Once validated, the numerical model might serve as basis for the development of the digital twin of the staircase. Furthermore, deformable treads (interacting with contact laws) are considered for the first time, allowing for stress and strain analyses. Particularly, the stress flows and distributions appear more informative on the structural behavior than simple reaction forces (e.g., torque) in such complex structures. Finally, beyond showing the dependency of the results on various parameters, the experimental data obtained under controlled loading are used as reference to identify the most plausible actual boundary conditions of the treads in the staircase and explain its overall structural behavior and outstanding performance.

3. Monitoring and numerical modeling

3.1. Museum of the City of New York staircase

The cantilever staircase in the Museum of the City of New York (MCNY), composed of 36 marble treads, is adopted as case study due to its impressive slenderness and availability. Located at 1220 Fifth Avenue in Manhattan, the museum is currently housed in a neo-Georgian building designed by Joseph H. Freelander and completed in 1932. The semicircular cantilever staircase in the main rotunda is a central feature of the building and a graceful example of this structural system. MCNY recently completed a decade-long renovation project that included structural changes to the staircase, where a curved I-beam was installed to replace the segment of supporting wall that was removed to create two new openings, one for a window and another for a doorway (Fig. 2). The MCNY staircase is composed of triangular cross-section treads with rounded mortared connections (Fig. 2), made of Imperial Danby marble.

3.2. Strain monitoring and loading conditions

In the framework of the structural health monitoring (SHM, [26–28]) of the staircase, seven fiber-optic strain sensors were initially installed on the soffit of the stair treads, and only three sensors are relevant for this study. Simple bare Fiber Bragg Grating (FBG) fiber-optic strain sensors consisting of single polyimide-coated FBG were used. The sensors were prestressed and glued at the two ends to the marble treads. In particular, a silane moisture-curing polymer (Loctite Go2® Gel) was utilized as adhesive, being completely and easily removable from marble substrates. The clear distance between the glued ends of each sensor, i.e., the gauge length of each sensor, was 10 cm. The repeatability precision of the sensor was evaluated to 0.1 $\mu\varepsilon$. Given that all tests were performed indoors, in a short term (less than 30 min per test), the temperature during the test was considered constant and there was no need for thermal compensation of the sensors [29,30]. However, small thermal variations in the air next to sensors could affect the measurements and introduce inaccuracy; nevertheless, they were estimated to be less than 0.1 °C in absolute value, resulting in an error of ± 0.8 $\mu\varepsilon$. This error, combined with the repeatability precision of the sensor, resulted in limits of error or approximately ± 1.0 $\mu\varepsilon$. As the geometry of the treads is repeated uniformly, one tread only is considered as representative. Particularly, the fifteenth tread from the bottom is selected as representative and the three considered sensors are directly attached to it, see Fig. 3 (top).

Sensors 1 is installed along the axis of the tread length on the line that bisects the soffit to measure strain induced by bending. It is installed at a third of the distance from the free end. Sensor 2 and Sensor 3 are oriented 45° to the bisecting line, and 90° relative to each other, closest to the fixed end, and crossing the decorative indent as shown in the magnified portion in Fig. 3. This crossed topology is expected to be sensitive to both shear and torsion.

A group of sixteen Princeton students (Fig. 3) volunteered to apply different loading schemes to the staircase. In particular, two load cases (labeled as LC-DOWN and LC-UP) have been considered. In LC-DOWN, four subgroups of four students with similar cumulative weight were identified, while in LC-UP four subgroups of two students of similar cumulative weight were identified (Table 1). Each subgroup was expected to stand on a single tread. In LC-DOWN, the four students of each subgroup were distributed along the full length of the tread, while in LC-UP the two students of each subgroup were distributed only on the half-length closer to the free end. In LC-DOWN, the subgroups started from the top of the stairs and moved one step down at a time in subsequent treads, until the last subgroup stepped off. In LC-UP, the subgroups started from the bottom of the stairs and moved one step up at a time in subsequent

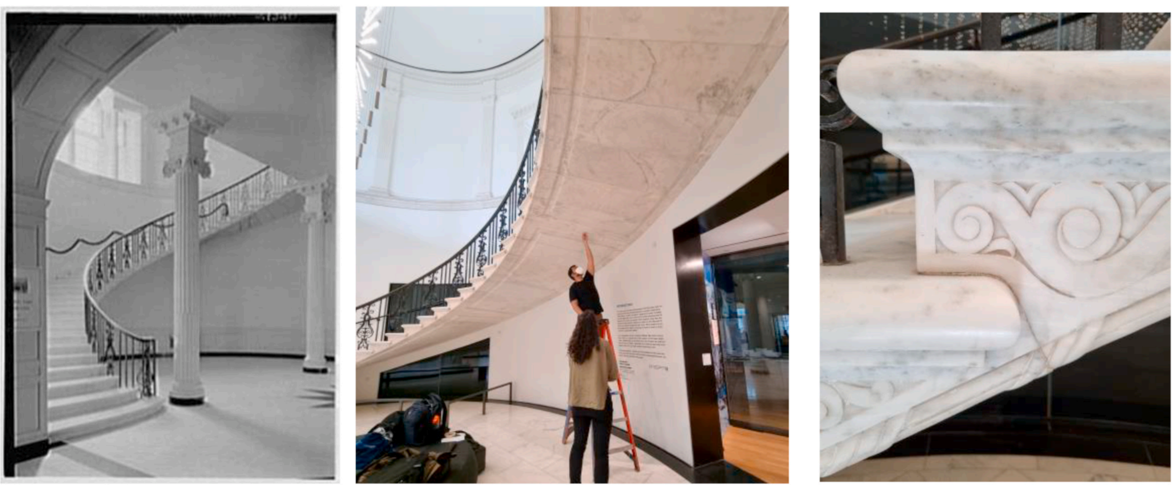

Fig. 2. The Museum of the City of New York staircase. Historic photograph (left, credit: Samuel H. Grottscho, 1934, Gottscho-Schleisner Collection, Library of Congress, Prints and Photographs Division), installation of sensors (center), detail of the treads connection (right).

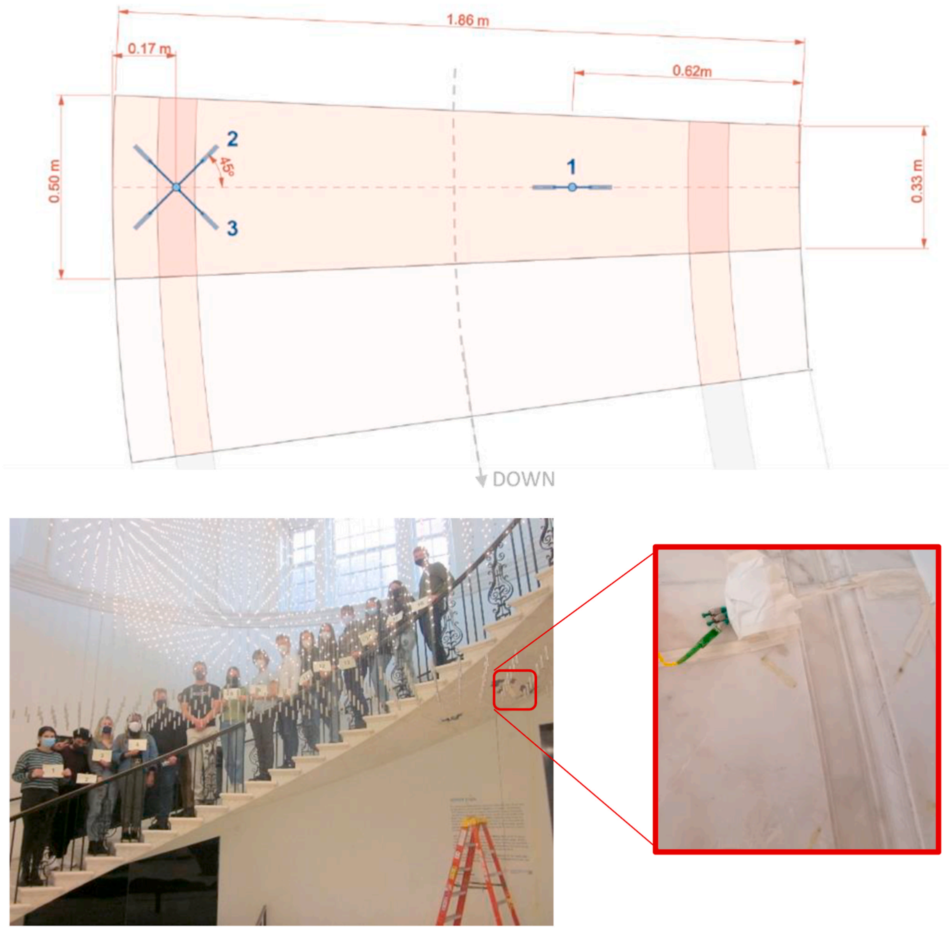

Fig. 3. Sensors distribution on the fifteenth tread (top) and example of human load (bottom), with a magnified portion showing the cross-topology sensors.

Table 1
Weights involved in the load cases.

Load case	Subgroup 1	Subgroup 2	Subgroup 3	Subgroup 4
LC-DOWN	270 kg	274 kg	276 kg	297 kg
LC-UP	171 kg	168 kg	166 kg	159 kg

treads. Before moving any step down or up, fiber optic strain measurements were collected. In the following, the strain data recorded by means of FBG fiber-optic sensors are referred to as experimental data.

3.3. Numerical modeling

A finite element model of the entire staircase, where each tread is idealized as a 3D solid deformable body interacting with the adjacent ones through contact-based interactions, is developed (Fig. 4). The first and the last treads of the staircase have not been modeled as fixed to the floors, and clamped boundary conditions have been adopted on the surfaces of the treads adjacent to the non-modeled treads. Each tread is discretized by means of 2302 four-node tetrahedral finite elements with linear shape functions on edges (average mesh size equal to 4.6 cm), adopting a linear elastic isotropic constitutive law. A Lagrange multiplier contact method, characterized by "hard" contact and frictional response, is enforced between the treads by means of a node-to-surface master-slave contact formulation. The mechanical characterization has been carried out by considering Imperial Danby marble properties, i.e. 70 GPa for Young's modulus, 0.2 for Poisson's ratio, and 2700 kg/m^3 for material density, as well as a friction coefficient equal to 0.6, which accounts for the mortared connections between treads. It appears worth to mention that preliminary analyses highlighted a negligible influence of the friction coefficient on the results.

The complex rounded mortared connections between treads (Fig. 2, right) have been simplified by two surfaces with a sharp angle. The artistic indent highlighted in Fig. 3 has been explicitly inserted only in the considered tread (fifteenth tread) for the sake of simplicity. Based on the construction details of the staircase, it is not clear whether the connection between the treads and the wall is fully fixed, flexibly fixed, or simply supported (pinned). Also, there is possibility that some treads have fully fixed ends, some flexibly

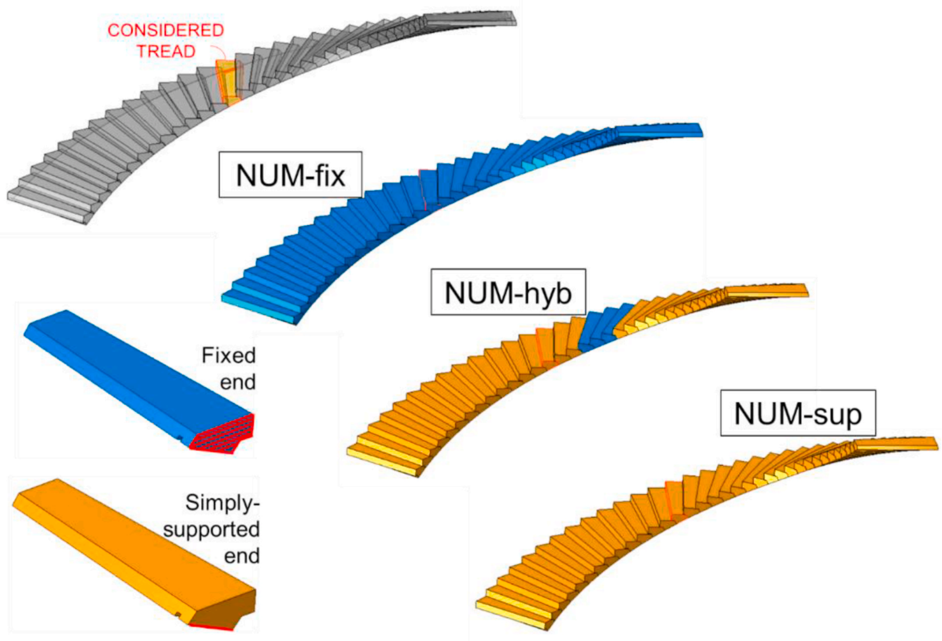

Fig. 4. Numerical model and boundary conditions.

fixed ends, and some simply supported ends. Creating numerical models that can simulate all possible scenarios would be impractical (for example, if we consider only fixed-end and pinned connections, the total number of models would be $2^{36} > 1000000000$). Thus, to get insights on structural behavior of staircase, while keeping the analysis simple, only three different boundary conditions have been considered for the model (Fig. 4). In particular, the case NUM-fix conceives fixed-end boundary conditions at the wall, while the case NUM-sup adopted simply supported (pinned) boundary condition at the wall end, as highlighted in Fig. 4 (the red lines highlight the positions of the nodes where all the spatial displacements have been restrained). Beyond these two extreme cases, the hybrid case NUM-hyb is also considered. It is characterized by all simply supported treads with the exception of the three treads above (but not adjacent to) the considered one, which were modeled with fixed-end conditions. Although this case has not a direct physical link to the real staircase, it is here used to show whether variations in the structural response can be observed while varying the boundary conditions over a few treads close (but not adjacent to) the considered tread. Multi-step static nonlinear analyses are performed by changing the loads position at each step to reproduce the load sequence (in the further text referred to as pseudo-time) of the experiment. The load cases are simulated by means of vertical pressure loads distributed on the top surface of each tread, with different pseudo-time histories for each tread set to reproduce the experimental load sequence. Moreover, in LC-DOWN the pressure is distributed on the full top surface of the tread, while in LC-UP the pressure is distributed only on the half-surface closer to the free end. Numerical strain data are derived from the displacements extracted in the positions in which the sensors were glued to the tread.

4. Results and discussion

The comparison between experimental and numerical results is shown in Fig. 5 in terms of strain measurements along with the load sequence for both LC-DOWN and LC-UP. Firstly, it is worth highlighting a few aspects of the experimental response. All strain measurement magnitudes are very low, below 8 $\mu\varepsilon$ (i.e., very small strains in general). Sensor 1 shows a positive strain peak at around pseudo-times 22 and 15 for LC-DOWN and LC-UP, respectively (i.e., when students are just above the considered tread), while the rest of the response shows an almost-null strain. Accordingly, the tread is subjected to tension in the location of Sensor 1, which is a condition far from the hypothesis of cantilever beam. Sensor 2 and Sensor 3 show strain measurements much higher than Sensor 1 (Fig. 5). Negative strain peaks are measured by Sensor 2 at around pseudo-time 24 (13) for LC-DOWN (LC-UP), being the response up to pseudo-time 20 (after pseudo-time 18) with almost-null strain. Sensor 3 shows a change of strain sign in both LC-DOWN and LC-UP, being the magnitude of positive and negative peaks comparable. Given the inclination of the tread soffit, the aspect of non-symmetrical sensors response between Sensor 2 and Sensor 3 appears reasonable.

By comparing the experimental results with the numerical ones for Sensor 1, both NUM-sup and NUM-hyb show positive strain peaks in agreement with the experimental ones (for both LC-DOWN and LC-UP), while the case NUM-fix shows extremely small strains that change sign repeatedly. The comparison for Sensor 2 shows that NUM-fix is the only case that does not show any change of sign in the response. This agrees with the experimental response, although the case NUM-hyb shows a main negative strain peak preceded (followed) by a much smaller positive strain peak for LC-DOWN (LC-UP). Conversely, NUM-sup shows significant positive strains before (after) the negative strain peak for LC-DOWN (LC-UP), showing a response rather far from the experimental one. Finally, the comparison for Sensor 3 shows that the only case which is able to show a change of strain sign with positive and negative

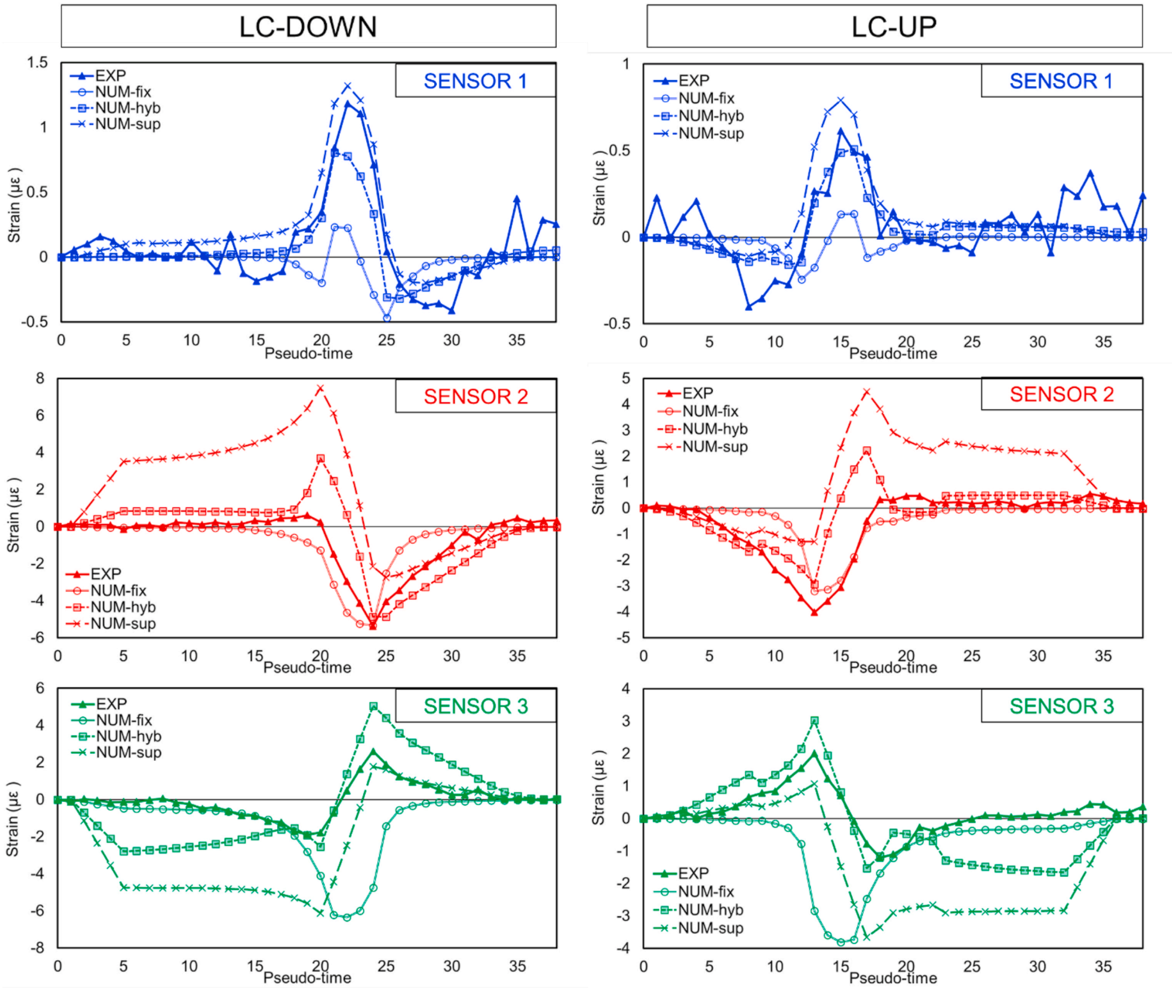

Fig. 5. Results comparison: LC-DOWN (left) and LC-UP (right). The pseudo-time is an indication of the load sequence.

strain peaks comparable in magnitude is NUM-hyb, as NUM-fix shows only negative strain measurements and NUM-sup is characterized by magnitudes of negative strain much higher than positive ones, for both LC-DOWN and LC-UP cases. Hence, the case NUM-hyb characterized by hybrid boundary conditions appears to better fit the experimental response for the three sensors, for both load cases. Indeed, while the limits of error of strain measurements (± 1 με) are relatively high compared with the measured strain (< 8 με), only in the case NUM-hyb the difference between the measured strain and the modeled strain is almost systematically within the limits of error. Some discrepancies were noted, and they can be attributed to the limitations in simulating the real boundary conditions, which may be different from those accounted in the models. However, further tuning boundary conditions in the model for each tread to perform full structural identification would require much more extensive analysis, which would lead to better agreement between measurements and the model but would not significantly add to the insights resulting from the analysis performed in this paper.

Beyond the extraction of strain measurements, the adopted numerical modeling approach allows to gather additional information about the contact stresses between treads (Fig. 6, with a color scale limited to 2 MPa to highlight the differences) and stress distributions along the treads (Fig. 7, with a color scale limited to −4 MPa to highlight the differences). In particular, the contact stresses between treads due to dead load are shown in Fig. 6 for NUM-fix, NUM-hyb, and NUM-sup. As it can be noted, contact stresses between treads tend to be concentrated close to the free extremity, being much higher in NUM-sup and NUM-hyb than in NUM-fix. Accordingly, the structural condition of the treads in NUM-sup and NUM-hyb is far from the hypothesis of cantilever beam, as also highlighted by the response of Sensor 1 that measures tension instead of compression (which would be the case of a cantilever scheme). The minimum principal stress contour plots for NUM-fix, NUM-hyb, and NUM-sup at pseudo-time 20 is shown in Fig. 7 for the case LC-DOWN. As it can be observed, no significant compressive stress flow is shown by NUM-fix, while a clear compressive stress flow is observed close to the free end in both NUM-sup and NUM-hyb (the latter showing higher compressive stresses in the intrados of fixed-end treads). Such compressive stress flow which goes from the top to the bottom is highlighted with a green-to-blue trace close to the free end in Fig. 7 for both NUM-sup and NUM-hyb.

The results show important insights into the structural behavior of the stone cantilever stair. In the cases where the treads are not systematically connected to the wall via full fixed-end connection (which is the most realistic case), the treads exhibit a behavior that

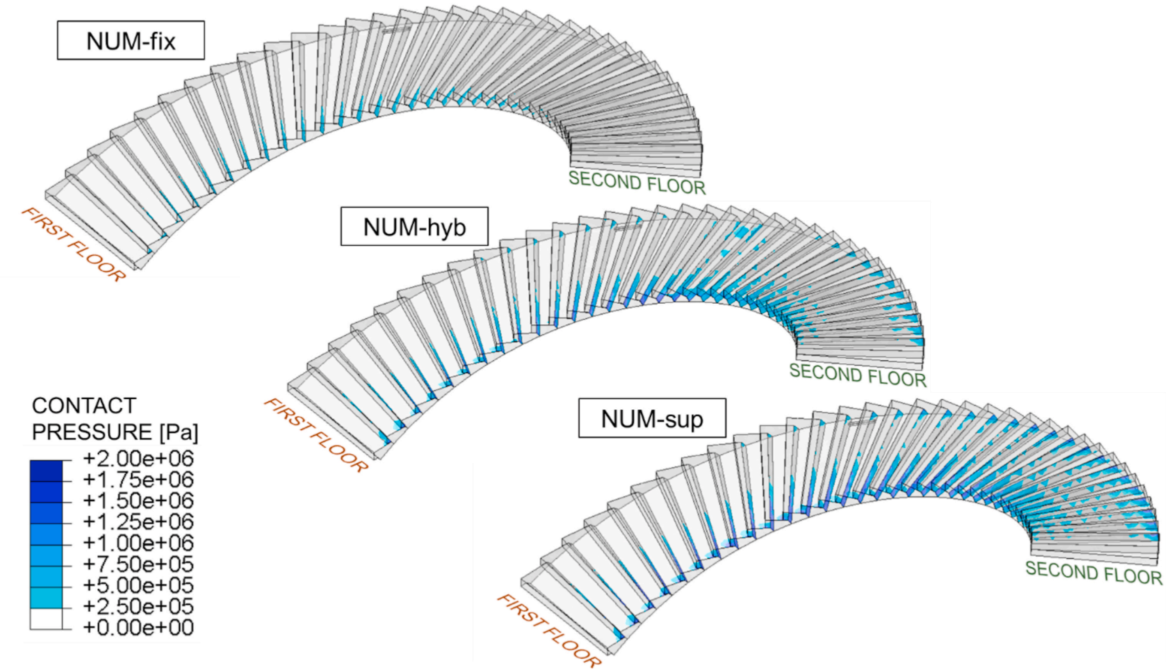

Fig. 6. Contact stresses (pressure) between treads due to dead load, top view.

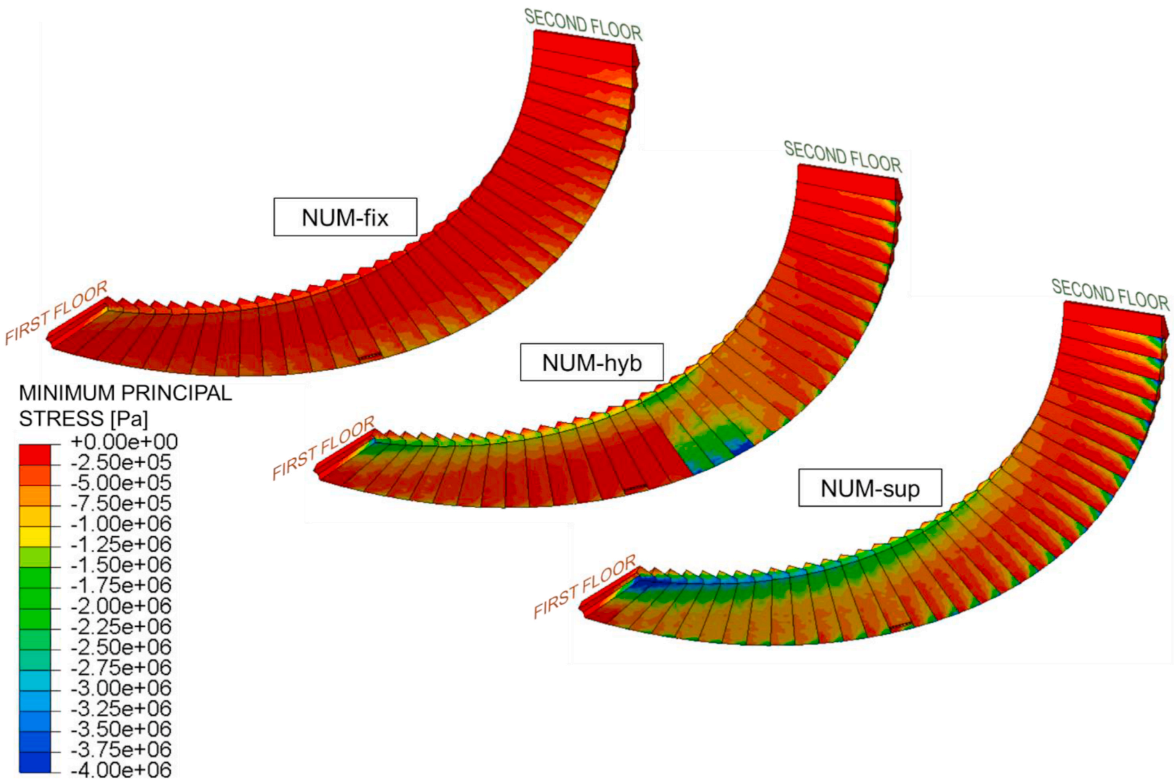

Fig. 7. Minimum principal stress contour plots at pseudo-time 20 (LC-DOWN), bottom view.

is similar to a beam having, in addition to the connection to the wall, a simple support close to the free end, i.e., at location where the maximum contact stress occur. Given that the maximum contact stress occurs between the observed tread and both upper and lower adjacent treads, they result in unbalanced forces that generate torsion in the tread. The force from the upper tread (i) is transmitted to the considered tread, and part of this force is taken by the lower tread (ii) along with part of the force coming from the load applied to the considered tread (iii). Thus, only the imbalance from these three forces is taken by the considered tread and carried to the connection to the wall, resulting in bending moments, shear forces, and torsional moment. Reducing the loading in treads (by transmitting part of it to lower tread, i.e., by transferring it successively from tread to tread all the way down to the basis) and engaging torsion in treads, both contribute to reducing stresses in treads, and explains their great structural performance, i.e., excellent load-carrying capacity.

5. Conclusions

In this paper, the structural behavior of a stone cantilever staircase has been investigated through an integration of strain monitoring and numerical modeling. The Museum of the City of New York staircase, composed of marble treads, served as a case study. This application represents the first ever integration of numerical modeling with actual strain measures on a historic cantilever staircase, with unknown actual boundary conditions, subjected to controlled loading. Fiber-optic sensors were installed in the intrados of a representative tread and experimental stain data were collected under moving human loads, with different loading schemes. Beyond the discussion of the experimental results, this paper aimed to validate quantitatively a numerical model of the staircase through experimental data. To this end, a 3D finite element model of the whole staircase based on contact interactions, has been used to simulate the loading cases considering various boundary conditions. The comparison between experimental and numerical results allowed to identify the most plausible actual boundary condition of the treads, given the good agreement of results obtained. Accordingly, the numerical model might serve as basis for the development of the digital twin of the staircase. Innovatively, deformable treads interacting with contact laws were concerned, allowing for stress and strain analysis of the staircase. Such results deepened the knowledge of the structural behavior of these complex cultural heritage structures, and they appeared sufficiently accurate given the agreement with experimental outcomes.

CRediT authorship contribution statement

Antonio Maria D'Altri: Writing – original draft, Supervision, Software, Methodology, Funding acquisition, Data curation, Conceptualization. **Yolanda Jin:** Validation, Investigation, Data curation. **Jessica Chen:** Validation, Software, Data curation. **Tiffany Agyarko:** Validation, Software, Data curation. **Guy Nordenson:** Writing – review & editing, Supervision, Resources. **Branko Glisic:** Writing – review & editing, Supervision, Resources, Project administration, Methodology, Investigation, Funding acquisition, Conceptualization.

Declaration of competing interest

The authors declare that they have no known competing financial interests or personal relationships that could have appeared to influence the work reported in this paper.

Data availability

Data will be deposited in an Open Data repository

Acknowledgements

This project has received funding from the European Union's Horizon 2020 research and innovation programme under the Marie Sklodowska-Curie grant agreement No 101029792 (HOLAHERIS project, "A holistic structural analysis method for cultural heritage structures conservation"). The authors would like to thank Moriah Huges, Mauricio Pereira, Antti Valkonen, and the undergraduate students of CEE 312 Statics of Structures for the help in the data collection. Prof Rebecca Napolitano is also gratefully acknowledged for providing supervision to Yolanda Jin and Moriah Hughes for providing supervision to Jessica Chen. We would like to extend our gratitude to Patricia Zedalis, Henry Galindo, Daniel Curtin, and the entire team of the Museum of the City of New York whose support and kind collaboration were crucial for the success of the project.

References

[1] G. Nordenson, Reading Structures: 39 Projects and Built Works, Lars Müller Publishers, Zürich, 2016.
[2] A. Dell'Endice, M.J. DeJong, T. Van Mele, P. Block, Structural analysis of unreinforced masonry spiral staircases using Discrete Element modelling, Structures 46 (2022) 214–232.
[3] B. Rigó, K. Bagi, Discrete element analysis of stone cantilever stairs, Meccanica 53 (2018) 1571–1589.
[4] J.W. Campbell, M. Tutton, Staircases: History, Repair and Conservation, Routledge, London, 2013.
[5] S. Price, H. Rogers, Stone cantilevered staircases, Struct. Eng. 83 (2) (2005) 29–36.
[6] S.S. Kaushal, M.G. Soto, R. Napolitano, Understanding the performance of historic masonry structures in mayfield, KY after the 2021 tornadoes, J. Cult. Herit. 63 (2023) 120–134.
[7] F. Clementi, V. Gazzani, M. Poiani, S. Lenci, Assessment of seismic behaviour of heritage masonry buildings using numerical modelling, J. Build. Eng. 8 (2016) 29–47.
[8] A.M. D'Altri, G. Castellazzi, S. de Miranda, A. Tralli, Seismic-induced damage in historical masonry vaults: a case-study in the 2012 emilia earthquake-stricken area, J. Build. Eng. 13 (2017) 224–243, https://doi.org/10.1016/j.jobe.2017.08.005.
[9] J. Heyman, The mechanics of masonry stairs, in: Structural Studies of Historical Buildings, Computational Mechanics Publications, Southampton, 1995, pp. 259–265.
[10] P. Block, Thrust Network Analysis: Exploring Three-Dimensional Equilibrium, Doctoral dissertation, Massachusetts Institute of Technology, 2009.
[11] M. Angelillo, Static analysis of a Guastavino helical stair as a layered masonry shell, Compos. Struct. 119 (2015) 298–304.
[12] M. Angelillo, The equilibrium of helical stairs made of monolithic steps, Int. J. Architect. Herit. 10 (6) (2016) 675–687.

[13] A. Gesualdo, C. Cennamo, A. Fortunato, G. Frunzio, M. Monaco, M. Angelillo, Equilibrium formulation of masonry helical stairs, Meccanica 52 (2017) 1963–1974.
[14] M. Angelillo, C. Olivieri, M.J. DeJong, A new equilibrium solution for masonry spiral stairs, Eng. Struct. 238 (2021) 112176.
[15] C. Olivieri, A. Iannuzzo, A. Fortunato, M.J. DeJong, The effect of concentrated loads on open-well masonry spiral stairs, Eng. Struct. 272 (2022) 114952.
[16] F. De Serio, M. Angelillo, A. Gesualdo, A. Iannuzzo, G. Zuccaro, M. Pasquino, Masonry structures made of monolithic blocks with an application to spiral stairs, Meccanica 53 (2018) 2171–2191.
[17] C. Olivieri, S.C.C. Adriaenssens, A novel graphical assessment approach for compressed curved structures under vertical loading, Int. J. Space Struct. 38 (2) (2023) 141–155.
[18] A. D`Altri, V. Sarhosis, G. Milani, J. Rots, S. Cattari, S. Lagomarsino, E. Sacco, A. Tralli, G. Castellazzi, S. de Miranda, Modeling strategies for the computational analysis of unreinforced masonry structures: review and classification, Arch. Comput. Methods Eng. 27 (2020) 1153–1185.
[19] A. Cutolo, F. Guarracino, C. Olivieri, I. Mascolo, Nonlinear FE analysis of a masonry spiral staircase in Nisida: a refined numerical case study, Int. J. Multiscale Comput. Eng. 20 (5) (2022) 105–114.
[20] S. Szabó, M.F. Funari, P.B. Lourenço, Masonry patterns' influence on the damage assessment of URM walls: current and future trends, Develop.in the Built Environ. (2023) 100119.
[21] A.L. Monaco, N. Grillanda, I. Onescu, M. Fofiu, F. Clementi, M. D'Amato, A. Formisano, G. Milani, M. Mosoarca, Seismic assessment of Romanian Orthodox masonry churches in the Banat area through a multi-level analysis framework, Eng. Fail. Anal. 153 (2023) 107539.
[22] M. Schiavoni, E. Giordano, F. Roscini, F. Clementi, Advanced numerical insights for an effective seismic assessment of historical masonry aggregates, Eng. Struct. 285 (2023) 115997.
[23] G. Angjeliu, G. Cardani, D. Coronelli, T. Boothby, Modelling and safety assessment of observed sliding damage in a masonry rib vault, J. Cult. Herit. 59 (2023) 264–273.
[24] A. Ferrante, D. Loverdos, F. Clementi, G. Milani, A. Formisano, S. Lenci, V. Sarhosis, Discontinuous approaches for nonlinear dynamic analyses of an ancient masonry tower, Eng. Struct. 230 (2021) 111626.
[25] A. Ferrante, M. Schiavoni, F. Bianconi, G. Milani, F. Clementi, Influence of stereotomy on discrete approaches applied to an ancient church in Muccia, Italy, J. Eng. Mech. 147 (11) (2021) 04021103.
[26] M. Mishra, P.B. Lourenço, G.V. Ramana, Structural health monitoring of civil engineering structures by using the internet of things: a review, J. Build. Eng. 48 (2022) 103954.
[27] M.C. Porcu, E. Montis, M. Saba, Role of model identification and analysis method in the seismic assessment of historical masonry towers, J. Build. Eng. 43 (2021) 103114.
[28] E. García-Macías, e F. Ubertini, «Real-time Bayesian damage identification enabled by sparse PCE-Kriging meta-modelling for continuous SHM of large-scale civil engineering structures, J. Build. Eng. 59 (2022) 105004.
[29] N. Cavalagli, A. Kita, V.L. Castaldo, A.L. Pisello, F. Ubertini, Hierarchical environmental risk mapping of material degradation in historic masonry buildings: an integrated approach considering climate change and structural damage, Construct. Build. Mater. 215 (2019) 998–1014.
[30] E. García-Macías, F. Ubertini, Least Angle Regression for early-stage identification of earthquake-induced damage in a monumental masonry palace: Palazzo dei Consoli, Eng. Struct. 259 (2022) 114119.